Asian Journal of Chemistry; Vol. 38, No. 7 (2026), 1825-1832
ASIAN JOURNAL OF CHEMISTRY
https://doi.org/10.14233/ajchem.2026.36102

Synthesis, Spectral Characterisation and Docking Analysis of Thiazole-Based Schiff Base Derivatives as Novel Antimicrobial and Antifungal Agents

M. LOKHANDE, D. WAGARE, M. ADHYAPAK, B. SHELKE and S. PAWAR*,

Department of Chemistry, Vivekanand Arts, Sardar Dalipsingh Commerce and Science College, Chhatrapati Sambhajinagar-431001, India

*Corresponding author: E-mail: sangeetapawarvca@gmail.com

Received: 30 March 2026 *Accepted*: 4 June 2026 *Published online*: 3 July 2026 AJC-22408

A novel series of thiazole-based Schiff base derivatives (**ML-1** to **ML-10**) were synthesised *via* condensation of 2-aminothiazole with *N-Boc*-protected amino acids, followed by deprotection and reaction with various aromatic aldehydes. Structures were confirmed by FT-IR, ^{1}H NMR, ^{13}C NMR and mass spectrometry. The antibacterial activity of all the compounds was evaluated against six bacterial strains, showing that **ML-9** exhibited the strongest activity, with **ML-9** exhibiting the strongest activity, showing MIC values within the range of ciprofloxacin against selected strains. The antifungal activity was also assessed against *Fusarium oxysporum*, *Rhizoctonia solani* and *Colletotrichum capsici*, with **ML-9** showing the most potent inhibition with **ML-9** showing the lowest MIC values, approaching those of fluconazole against *Rhizoctonia solani* and *Colletotrichum capsici*. SAR studies highlighted the importance of electron-donating and -withdrawing groups in enhancing activity. Molecular docking against CYP51 (PDB ID: 4WMZ) revealed strong binding for **ML-9** and **ML-8** (G-scores: -6.735 and -6.560 kcal/mol), with stable interactions involving LEU380, PHE384 and TYR140. These results identify **ML-9** and **ML-8** as promising preliminary candidates for further structural optimisation and biological evaluation.

Keywords: Thiazole, Schiff base, Biological activity, Minimum inhibitory concentration, Molecular docking.

INTRODUCTION

The 4,5-dihydrothiazol-2-amine scaffold represents a significant heterocyclic framework in medicinal chemistry, owing to its synthetic accessibility and broad pharmacological potential. It is readily accessed *via* cyclocondensation of *N*-aryl thioureas with 2-haloethylamines, as well as through alternative heterocyclisation strategies; enantioselective routes to chiral analogues have also been reported [1,2]. A wide range of derivatives have demonstrated promising biological activities, encompassing antimicrobial, antithrombotic, anticancer and enzyme inhibitory properties [1,3-5]. Recent studies integrating synthetic work with crystallographic analysis, molecular docking and QSAR approaches have provided valuable insights into structure-activity relationships [3,5]. Reviews on 2-aminothiazole and related derivatives emphasize the privileged role of this nucleus in drug discovery and justify its continued exploration [4,6].

Similarly, Schiff bases derived from thiazole and dihydrothiazole scaffolds have been widely investigated for their structural diversity and biological significance. Phenylthiazole-hydroxybenzaldehyde Schiff bases have demonstrated therapeutic promise through theoretical and pharmacological evaluation [6]. Metal complexes of 2-amino-4-substituted phenylthiazole Schiff bases have shown significant biological activity, highlighting the importance of Schiff base ligands in coordination chemistry [7]. Schiff bases of 2-aminothiazoles have displayed strong anti-tubercular activity, supported by docking analyses [8], while derivatives of 2-amino-5-nitrothiazole and their thiazolidinone analogues have exhibited potential as anti-Alzheimer agents *via* cholinesterase inhibition [9]. Furthermore, the biological performance of thiazole-based Schiff bases is strongly influenced by the structural variation of the aldehyde component, particularly in antimicrobial studies [10]. The design and synthesis of new antimicrobial agents based on the 4,5-dihydrothiazol-2-amine scaffold remains an active area of research due to the privileged role of this nucleus in medicinal chemistry [11,12].

Schiff bases have been prepared by a variety of methods because of their wide applications in medicine, catalysis and materials science. The classical approach involves the condensation of aromatic aldehydes with primary amines under reflux,

typically in the presence of acidic or basic catalysts in organic solvents. Although simple, this method often suffers from drawbacks such as long reaction times, moderate yields and the use of volatile or costly solvents, raising safety and environmental concerns [13]. To address these issues, greener alternatives have been developed. Natural acids, including lemon juice, fruit extracts and anacardic acid, have been employed as eco-friendly catalysts due to their biodegradability and low toxicity. Inorganic systems such as Fe(III)-Mg-Al layered double hydroxide (Fe(III)MgAl-LDH), cerium(III) chloride heptahydrate, calcium oxide and P_2O_5 supported on alumina (P_2O_5/Al_2O_3) have demonstrated strong catalytic activity and stability [14-20]. Solid acids like montmorillonite K-10, a naturally occurring clay, is also effective, while conventional mineral acids such as HCl continue to be widely applied for their strong Brønsted acidity [21,22].

While thiazole-based Schiff bases have been previously reported, a gap persists in understanding the extent to which systematic aromatic substitutions influence antimicrobial behaviour, with most existing studies reporting activity without correlating structural features to possible modes of action. The novelty of this work lies in the development of a structurally distinct thiazole-Schiff base framework integrating a 4,5-dihydrothiazol-2-amine moiety with an amino acid-derived propanamide unit through microwave-assisted amide coupling. This molecular architecture remains scarcely explored in the literature. Comprehensive SAR studies, supported by antibacterial and antifungal MIC evaluations and molecular docking against CYP51, demonstrate that the potent activity of compounds **ML-9** and **ML-8**, comparable to standard drugs, originates from the combined influence of scaffold architecture, electronic effects, and favourable target interactions. These findings provide valuable insights for the rational development of thiazole-based antimicrobial agents.

EXPERIMENTAL

All chemicals and reagents were obtained from commercial suppliers (TCI Chemicals and Avra Laboratories) and used without further purification. The progress of reactions was monitored by thin-layer chromatography (TLC) using pre-coated silica gel 60 F_{254} aluminium plates (Merck). TLC spots were visualised under ultraviolet (UV) light. ^{1}H and ^{13}C NMR spectra were recorded on a Bruker spectrometer operating at 500 MHz for ^{1}H and 125 MHz for ^{13}C, using $CDCl_3$ as the solvent. Tetramethylsilane (TMS) was employed as the internal standard. ES-MS were acquired using a Waters Q-TOF micro mass spectrometer equipped with an electrospray ionisation (ESI) source.

Synthesis of (*S*)-2-amino-*N*-(4,5-dihydrothiazol-2-yl)-propanamide (4) (ML-amine): To a solution of (2*S*)-2-{[(*tert*-butoxy)carbonyl]amino}propanoic acid (**1**) (9.7 g, 0.0515 mol), carbonyldiimidazole (9.0 g, 0.0556 mol) in DCM (30 mL) was added in solution of 4,5-dihydrothiazol-2-amine (**2**) (5.0 g, 0.0490 mol) in DCM (30 mL) at 25-30 ºC and whole reaction mass was stirred for 3 h. The reaction was monitored by TLC (DCM:MeOH: 9:1), after completion, the reaction was quenched with water and product extracted with DCM. The organic layer was washed with 10% brine solution (400 mL) and after layer separation organic layer was concentrated at 45 ºC under vacuum, the obtained residue was suspended in methyl *tert*-butyl ether (MTBE). It was then filtered and dried to obtain *tert*-butyl (*S*)-1-(4,5-dihydrothiazol-2-ylcarbamoyl)ethylcarbamate (**3**) as white solid, yield (12.04 g, 90%). The product was confirmed by ES-MS. Compound **3** was dissolved in DCM (60 mL). To this solution, trifluoroacetic acid (25.3 g, 0.2216 mol) was added at 0-5 ºC, whole reaction was stirred for 3 h. The reaction was monitored by TLC (DCM:MeOH: 9:1), after completion, the reaction was quenched with aqueous 5% Na_2CO_3 solution to adjust pH 8-9 and product was extracted in DCM. The organic layer was washed with 10% brine solution (400 mL) and after layer separation organic layer was concentrated at 45 ºC under vacuum, to obtain (*S*)-2-amino-*N*-(4,5-dihydrothiazol-2-yl)propanamide (**4**) as yellowish-brown oily mass (6.5 g, 76%).

Synthesis of ML-1–ML-10 derivatives: To a solution of compound **4** (1.0 equiv.) and aromatic aldehyde (0.98 equiv.) in ethanol (5.0 times) were put in microwave reaction vessel equipped with a magnetic stirrer and irradiated at 560 W for 2-3 min. The reaction was monitored by TLC (DCM:MeOH: 9:1). After completion of reaction, cold water was added (20 times) to the reaction mixture. The product was extracted with DCM (5 times) and the organic layer was washed with 2% aqueous HCl (3 times), then concentrated under reduced pressure. The resulting residue was suspended in isopropyl ether (10 vol.), filtered and purified by column chromatography (ethyl acetate/hexane, 1:9 v/v) to afford **ML-1–ML-10** (**Scheme-I**).

(*S*)-2-Amino-*N*-(4,5-dihydrothiazol-2-yl)propanamide (4) (ML-amine): Yellowish brown; yield: 73.1%; ^{1}H NMR (400 MHz, $CDCl_3$, δ ppm): 8.23 (bs, 1H), 3.92-3.90 (t, 2H), 3.76 (s, 1H), 3.27-3.25 (t, 2H), 2.23 (bs, 2H), 1.23 (s, 3H); ^{13}C NMR (125 MHz, $CDCl_3$, δ ppm): 178.2, 161.2, 56.3, 49.7, 37.2, 24.2; ES-MS *m/z*: 174.1 (M + H) for $C_6H_{11}N_3OS$.

2-(4-Nitrobenzylideneamino)-*N*-(4,5-dihydrothiazol-2-yl)propanamide (ML-1): Light orange; yield: 85.2%; m.p.: 160-162 ºC; ^{1}H NMR (400 MHz, $CDCl_3$, δ ppm): 8.72 (s, 1H), 8.37 (s, 1H), 8.05-8.04 (d, 2H), 7.45-7.43 (d, 2H), 4.65 (s, 1H), 3.93-3.87 (d, 2H), 3.26-3.23 (d, 2H), 1.23 (s, 3H); ^{13}C NMR (100 MHz, $CDCl_3$, δ ppm): 179.161.4, 159.5, 150.2, 141.7, 130.9, 121.2, 55.5, 49.5, 35.2, 25.6; IR (KBr, ν_{max}, cm^{-1}): ESMS *m/z*: 307.0 (M + H) for $C_{13}H_{14}N_4O_3S$.

2-(4-Bromobenzylideneamino)-N-(4,5-dihydrothiazol-2-yl)propanamide (ML-2): White; yield: 86.3%; m.p.: 186-188 ºC; ^{1}H NMR (400 MHz, $CDCl_3$): 8.75 (s, 1H), 8.34 (s, 1H), 7.55-7.53 (d, 2H), 7.43-7.41 (d, 2H), 4.66 (s, 1H), 3.93-3.87 (d, 2H), 3.26-3.23 (d, 2H), 1.23 (s, 3H); ^{13}C NMR (125 MHz, $CDCl_3$, δ ppm): 179.1, 160.2, 159.6, 137.4, 130.5, 130.1, 126.8, 69.6, 55.6, 49.7, 35.2, 25.7; ES-MS *m/z*: 340.0 (M + H) for $C_{13}H_{14}BrN_3OS$.

***N*-(4,5-Dihydrothiazol-2-yl)-2-((4-methylbenzylidene)-amino)propanamide (ML-3):** Off white; yield: 88.2%; m.p.: 202-203 ºC; ^{1}H NMR (400 MHz, $CDCl_3$, δ ppm): 8.70 (s, 1H), 8.35 (s, 1H), 7.51-7.49 (d, 2H), 7.10-7.08 (d, 2H), 4.65 (s, 1H), 3.93-3.87 (d, 2H), 3.26-3.23 (d, 2H), 2.18 (s, 3H), 1.25 (s, 3H); ^{13}C NMR (125 MHz, $CDCl_3$, δ ppm): 179.2, 161.2, 159.9, 142.2, 135.4, 128.3, 128.0, 127.9, 55.3, 49.9, 37.1, 27.3, 25.2; ES-MS *m/z*: 276.1 (M + H) for $C_{14}H_{17}N_3OS$.

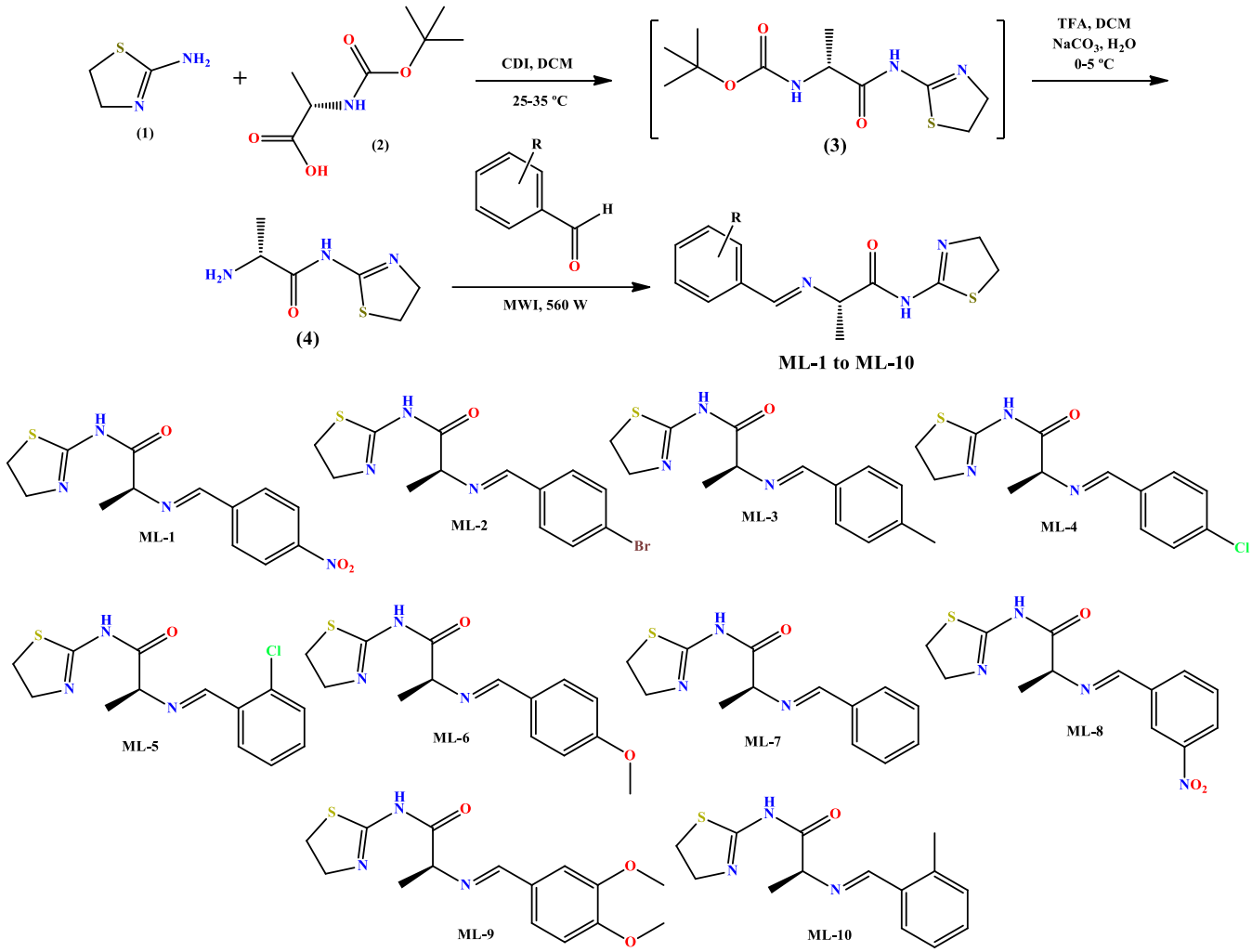

Scheme-I: Synthesis of thiazole-based Schiff base derivatives (**ML-1–ML-10**)

2-((4-Chlorobenzylidene)amino)-*N*-(4,5-dihydrothiazol-2-yl)propanamide (ML-4): Light yellowish; yield: 90.2%; m.p.: 238-239 ºC; ^{1}H NMR (400 MHz, $CDCl_3$, δ ppm): 8.72 (s, 1H), 8.32 (s, 1H), 7.57-7.55 (d, 2H), 7.18-7.16 (d, 2H), 4.69 (s, 1H), 3.92-3.86 (d, 2H), 3.25-3.22 (d, 2H), 1.25 (s, 3H); ^{13}C NMR (125 MHz, $CDCl_3$, δ ppm): 179.3, 161.3, 159.8, 140.2, 135.4, 130.0, 129.0, 55.3, 49.9, 37.1, 25.3; ES-MS *m/z*: 296.1 (M + H) for $C_{13}H_{14}ClN_3OS$.

2-((2-Chlorobenzylidene)amino)-*N*-(4,5-dihydrothiazol-2-yl)propanamide (ML-5): Light grey; yield: 85.9%; m.p.: 226-227 ºC; ^{1}H NMR (400 MHz, $CDCl_3$, δ ppm): 8.73 (s, 1H), 8.38 (s, 1H), 7.62-7.61 (d, 1H), 7.29-7.28 (d, 1H), 7.05-6.98 (m, 2H), 4.69 (s, 1H), 3.93-3.87 (d, 2H), 3.26-3.23 (d, 2H), 1.25 (s, 3H); ^{13}C NMR (125 MHz, $CDCl_3$, δ ppm): 179.1, 160.3, 159.6, 139.2, 137.5, 130.5, 129.9, 69.6, 55.5, 49.7, 35.5, 25.7; IR (KBr, ν_{max}, cm^{-1}): 1849 (C=O), 1644 (C=N), 1456 (C=C aromatic), 1167 (C-S), 775 (C-Cl); ES-MS *m/z*: 296.1 (M + H) for $C_{13}H_{14}ClN_3OS$.

***N*-(4,5-Dihydrothiazol-2-yl)-2-((4-methoxybenzylidene)-amino)propanamide (ML-6):** Off white; yield: 84.3%; m.p.: 176-177 ºC; ^{1}H NMR (400 MHz, $CDCl_3$, δ ppm): 8.70 (s, 1H), 8.36 (s, 1H), 7.52-7.50 (d, 1H), 6.81-6.79 (d, 2H), 4.66 (s, 1H), 3.93-3.87 (d, 2H), 3.26-3.23 (d, 2H), 1.23 (s, 3H); ^{13}C NMR (125 MHz, $CDCl_3$, δ ppm): 179.3, 164.2, 161.2, 159.7, 131.9, 130.0, 114.2, 57.0, 55.3, 49.9, 37.1, 25.3; IR (KBr, ν_{max}, cm^{-1}): 1644 (C=N), 1459 (C=C arom.), 1281 (O-CH_3), 1159 (C-S); ES-MS *m/z*: 292.1 (M + H) for $C_{14}H_{17}N_3O_2S$.

2-(Benzylideneamino)-N-(4,5-dihydrothiazol-2-yl)propanamide (ML-7): White; yield: 91.5%; m.p.: 201-202 ºC; ^{1}H NMR (400 MHz, $CDCl_3$, δ ppm): 8.71 (s, 1H), 8.37 (s, 1H), 7.62-7.60 (d, 1H), 7.32-7.27 (m, 3H), 4.63 (s, 1H), 3.93-3.87 (d, 2H), 3.26-3.23 (d, 2H), 1.25 (s, 3H); ^{13}C NMR (125 MHz, $CDCl_3$, δ ppm): 179.3, 160.2, 159.6, 137.4, 131.1, 130.0, 127.8, 69.6, 55.6, 49.7, 35.2, 25.7; IR (KBr, ν_{max}, cm^{-1}): 2920 (C-H, aromatic), 1644 (C=N), 1455 (C=C arom.), 1159 (C-S); ES-MS *m/z*: 262.1 (M + H) for $C_{13}H_{15}N_3OS$.

***N*-(4,5-Dihydrothiazol-2-yl)-2-((3-nitrobenzylidene)-amino)propanamide (ML-8):** Dark grey; yield: 93.7%; m.p.: 279-280 ºC; ^{1}H NMR (400 MHz, $CDCl_3$, δ ppm): 8.72 (s, 1H), 8.50-8.49 (d, 1H), 8.37 (s, 1H), 8.00-7.99 (d, 1H), 7.74-7.70 (m, 2H), 4.65 (s, 1H), 3.93-3.87 (d, 2H), 3.26-3.23 (d, 2H), 1.25 (s, 3H); ^{13}C NMR (125 MHz, $CDCl_3$, δ ppm): 179.2, 161.2, 148.0, 140.2, 135.2, 129.8, 121.9, 56.3, 49.7, 37.2, 25.2; IR (KBr, ν_{max}, cm^{-1}): 1645 (C=N), 1522, 1348 (NO_2); 1457 (C=C arom.), 1162 (C-S); ES-MS *m/z*: 307.1 (M + H) for $C_{13}H_{14}N_4O_3S$.

***N*-(4,5-Dihydrothiazol-2-yl)-2-((3,4-dimethoxybenzylidene)amino)propanamide (ML-9):** Light grey; yield: 92.4%; m.p.: 153-154 ºC; ^{1}H NMR (400 MHz, $CDCl_3$, δ ppm): 8.75 (s, 1H), 8.38 (s, 1H), 6.93-6.92 (d, 1H), 6.90 (s, 1H), 6.79-6.78 (d, 1H), 4.69 (s, 1H), 3.94-3.88 (d, 2H), 3.58 (s, 6H), 3.26-3.23 (d, 2H), 1.25 (s, 3H); ^{13}C NMR (125 MHz, $CDCl_3$, δ ppm): 179.3, 161.2, 159.7, 152.0, 149.5, 131.9, 122.2, 114.2, 57.1, 55.3, 49.9, 37.1, 25.3; IR (KBr, ν_{max}, cm^{-1}): 1646 (C=N), 1457 (C=C arom.), 1278 (O-CH_3), 1161 (C-S); ES-MS *m/z*: 322.1 (M + H) for $C_{15}H_{19}N_3O_3S$.

***N*-(4,5-Dihydrothiazol-2-yl)-2-((2-methylbenzylidene)amino)propanamide (ML-10):** Yellowish; yield: 89.5%; m.p.: 142-143 ºC; ^{1}H NMR (400 MHz, $CDCl_3$, δ ppm): 8.69 (s, 1H), 8.37 (s, 1H), 7.50-7.49 (d, 1H), 7.04-6.99 (m, 3H), 4.63 (s, 1H), 3.93-3.87 (d, 2H), 3.26-3.23 (d, 2H), 2.15 (s, 3H), 1.25 (s, 3H); ^{13}C NMR (125 MHz, $CDCl_3$, δ ppm): 179.2, 161.9, 159.4, 142.2, 135.3, 128.3 128.0, 127.9, 55.2, 49.9, 37.3, 27.3, 25.2; ES-MS *m/z*: 276.1 (M + H) for $C_{14}H_{17}N_3OS$.

Biological evaluation: The antibacterial and antifungal activities were evaluated under standardised conditions and all experiments were performed in triplicate. The results are expressed as mean ± standard deviation. Statistical comparison between the synthesised compounds and the standard drugs was carried out using one-way analysis of variance (ANOVA), followed by an appropriate post-hoc test to assess differences between individual compounds and the reference standards. A significance level of $p < 0.05$ was considered statistically significant. Based on the obtained results, the compounds demonstrated moderate biological activity and the results have been interpreted accordingly.

Antibacterial activity: The antibacterial activity of the synthesised compounds was evaluated using commercially prepared tryptic soya broth and malt extract broth [23]. The synthesised compounds were evaluated for their antibacterial activity against both Gram-negative (*Klebsiella aerogenes*, *Pseudomonas aeruginosa*, *Chromobacterium violaceum*) and Gram-positive (*Staphylococcus aureus*, *Lysinibacillus sphaericus*, *Bacillus subtilis*) bacterial strains using the minimum inhibitory concentration (MIC) method, with ciprofloxacin as the reference drug.

Antifungal activity: The antifungal activity was assessed using ready-made Mueller-Hinton agar medium [24]. The synthesised compounds **ML-1** to **ML-10** were evaluated for their antifungal activity against *Fusarium oxysporum*, *Rhizoctonia solani* and *Colletotrichum capsici* using the minimum inhibitory concentration (MIC) method, with fluconazole as the standard drug.

Molecular docking: Molecular docking was performed to evaluate the antifungal activity of target compounds by using Schrödinger software [25]. Before evaluating the biological activity, molecular docking studies were performed using the crystal structure 4WMZ, which represents Baker's yeast lanosterol 14α-demethylase (CYP51A1), a member of the cytochrome P450 superfamily, with fluconazole as the bound ligand.

RESULTS AND DISCUSSION

Although microwave-assisted Schiff base synthesis and aminothiazole chemistry are well-documented, the present study introduces a structurally distinct molecular framework by integrating a 4,5-dihydrothiazol-2-amine moiety, an amino acid-derived propanamide linker and a Schiff base pharmacophore into a single chiral scaffold. The synthesis of the novel thiazole-based Schiff base derivatives (**ML-1** to **ML-10**) was accomplished *via* the pathway as shown in **Scheme-I**. The synthesis of thiazole-based Schiff base derivatives (**ML-1** to **ML-10**) was initiated by the condensation of 2-aminothiazole (**1**) with *N*-*Boc*-L-alanine (**2**) using *N*,*N*′-carbonyldiimidazole (CDI) as the coupling reagent, affording intermediate (**3**) through amide bond formation. CDI activates the carboxylic acid to generate a reactive acylimid-azole intermediate, enabling efficient coupling under mild conditions. Subsequent deprotection of the Boc group under acidic conditions yielded the free amine intermediate **4**. Finally, condensation of intermediate **4** with various substituted aromatic aldehydes under microwave irradiation (560 W, 2-3 min) furnished the target Schiff base derivatives **ML-1** to **ML-10** in good yields. Compared with conventional reflux methods, microwave-assisted synthesis significantly reduced reaction times while maintaining satisfactory yields, likely due to rapid and uniform heating that minimizes side reactions and thermal degradation. The adopted microwave-assisted protocol provided an efficient and reproducible route for the synthesis of the target compounds.

N,*N*′-Carbonyldiimidazole (CDI) was selected as the coupling reagent for amide bond formation due to its efficiency and operational advantages over conventional reagents such as DCC and EDCI [26]. CDI activates the carboxylic acid through the formation of a reactive acyl-imidazole intermediate, facilitating coupling with 2-aminothiazole under mild conditions. In addition, CDI minimizes racemization at the α-carbon of the amino acid and generates readily removable byproducts (imidazole and CO_2), making it particularly suitable for the synthesis of chiral amino acid-derived intermediates [27]. *N*-*Boc*-L-alanine was employed as the chiral precursor to maintain the stereochemical configuration of naturally occurring L-amino acids, thereby preserving structural consistency and potential biological compatibility. The use of L-alanine also enabled systematic evaluation of the influence of aromatic substitutions on the antimicrobial activity of the synthesized derivatives, while exploration of alternative enantiomers was beyond the scope of the present study [28].

All target compounds (**ML-1** to **ML-10**) were obtained as stable crystalline solids and purified by recrystallization. The structural characterization was accomplished using FT-IR, ^{1}H NMR, ^{13}C NMR and mass spectrometry. FT-IR spectra displayed characteristic absorptions corresponding to the imine (C=N), amide (C=O/N–H) and thiazole-associated C–S functionalities, confirming the formation of the desired framework. The imine stretching band appeared around 1644 cm^{-1}, consistent with conjugated Schiff base systems, while the C–S stretching vibration was observed near 1167 cm^{-1} across the series. The ^{1}H NMR spectra showed the diagnostic azomethine proton signal (-CH=N-) and ^{13}C NMR spectra confirmed the presence of imine and amide carbonyl carbons. Furthermore, mass spectra exhibited molecular ion peaks in agreement with the calculated molecular masses of the synthesized compounds, providing additional confirmation of their structures

Antibacterial activity: The minimum inhibitory concentration (MIC) values of the synthesised compounds are shown in Table-1. All compounds share a common structural framework consisting of a heterocyclic core linked through an amide bond to a substituted aromatic ring. The antibacterial activity was found to be strongly influenced by the nature and position of substituents on the phenyl ring. Among the series, **ML-9** exhibited the highest potency, with MIC values ranging from 16-24 μg/mL. Its enhanced activity may be attributed to the presence of a dimethoxy-substituted aromatic ring, which increases lipophilicity and may facilitate improved membrane permeation and target interactions. **ML-8**, bearing a -NO_2 group, also demonstrated significant activity (18-26 μg/mL), while **ML-3** showed good potency, possibly due to reduced steric hindrance favouring target binding. In contrast, **ML-5** and **ML-6** displayed moderate antibacterial activity, whereas **ML-1**, **ML-2**, **ML-4** and **ML-7** were comparatively less active. **ML-10** showed the weakest activity (up to 32 μg/mL), which may be associated with increased steric bulk that limits effective interaction with bacterial targets.

Compared with ciprofloxacin (MIC: 19-29 μg/mL), **ML-8** and **ML-9** exhibited moderate antibacterial activity against selected microbial strains, particularly *C. violaceum*, *L. sphaericus* and *B. subtilis*. The structure-activity relationship analysis indicates that antibacterial activity is influenced by a combination of electronic, lipophilic and steric factors, with suitably positioned electron-withdrawing and lipophilic substituents contributing to improved activity. Among the synthesised derivatives, **ML-9** exhibited the most favourable antibacterial activity and may serve as a useful scaffold for further structural optimization and biological investigation.

Antifungal activity: Since all synthesised derivatives share the same heterocyclic–amide core, the differences observed in antifungal activity are likely associated with variations in the aromatic substituents. The antifungal results (Table-1) revealed that **ML-9** was the most active compound in the series, exhibiting MIC values of 10-14 μg/mL against the tested fungal strains. This enhanced activity may be related to the presence of an ester-containing substituent, which could improve physicochemical characteristics favourable for fungal target binding. Compounds **ML-8** and **ML-3** also exhibited appreciable antifungal activity, with MIC values of 12-16 μg/mL and 14-16 μg/mL, respectively; this activity may be attributed to the presence of electron-withdrawing substituents and reduced steric effects. Compounds **ML-5**, **ML-6** and **ML-7** displayed moderate antifungal effects, whereas **ML-4** was the least active derivative (MIC: 25-28 μg/mL). The lower activity observed for **ML-10** may be related to increased steric bulk, which could restrict effective interactions with fungal targets.

Compare to fluconazole (MIC: 15-19 μg/mL), compounds **ML-9**, **ML-8** and **ML-3** demonstrated favourable antifungal activity against certain fungal species, particularly *R. solani* and *C. capsici*. The structure–activity relationship suggests that antifungal efficacy is influenced by the combined effects of electronic properties, lipophilicity and steric factors, with appropriately positioned electron-withdrawing substituents generally associated with improved activity. Among the synthesized derivatives, **ML-9** displayed the most favourable antifungal profile and may serve as a useful scaffold for further optimization and antifungal evaluation.

Molecular docking: The molecular docking results of compounds **ML-1** to **ML-10** are shown in Table-2. The calculated binding energies ranged from -5.433 to -6.735 kcal mol^{-1}, reflecting moderate affinity toward the selected target protein. Among the series, **ML-9** (-6.735 kcal mol^{-1}) and **ML-8** (-6.560 kcal mol^{-1}) exhibited the most favourable docking scores. The binding pocket was predominantly composed of hydrophobic residues, including LEU380, LEU383, PHE384, VAL311, ILE139, TYR140 and LEU129, which accommodated the thiazole-based scaffold. Polar residues HIE381, SER382, SER508, THR318 and THR130 participated in hydrogen-bonding and electrostatic interactions that contributed to ligand stabilization. Hydrogen-bond interactions with MET509 and TYR126 were observed for **ML-3** and

TABLE-1
ANTIMICROBIAL ACTIVITY DATA OF SYNTHESISED THIAZOLE-BASED SCHIFF BASE DERIVATIVES (**ML-1** to **ML-10**)

Compounds	Minimum inhibitory concentration (μg/mL)								
	Antibacterial activity						Antifungal activity		
	Gram-negative bacteria			Gram-positive bacteria					
	K.A.	*P.A.*	*C.V.*	*S.A.*	*L.S.*	*B.S.*	*F.O.*	*R.S.*	*C.C.*
ML-1	30	28	26	30	28	26	21	15	18
ML-2	28	26	26	30	26	26	20	15	16
ML-3	22	22	20	24	20	21	16	14	14
ML-4	28	26	24	28	24	26	28	26	25
ML-5	24	22	21	24	22	23	19	13	17
ML-6	24	23	22	26	24	24	19	14	17
ML-7	26	24	24	28	22	26	18	14	16
ML-8	20	22	18	26	18	18	16	12	13
ML-9	18	20	16	24	16	16	14	12	10
ML-10	32	28	28	30	30	28	22	16	20
Ciprofloxacin	22	23	19	29	23	21	–	–	–
Fluconazole	–	–	–	–	–	–	19	15	17

K.A.: Klebsiella aerogenes; *P.A.: Pseudomonas aeruginosa*; *C.V.: Chromobacterium violaceum*; *S.A.: Staphylococcus aureus*; *L.S.: Lysinibacillus sphaericus*; *B.S.: Bacillus subtilis*; *F.O.: Fusarium oxysporum*; *R.S.: Rhizoctonia solani*; *C.C: Colletotrichum capsici.*
Negative control (DMSO): no activity.

TABLE-2
MOLECULAR DOCKING RESULTS OF THIAZOLE-BASED SCHIFF BASE DERIVATIVES (**ML-1** to **ML-10**) (PDB ID: 4WMZ)

Entry	G-Score	Binding energy	Residue			
			H-bond	Pi-pi stacking	Hydrophobic interactions	Polar interactions
ML-1	-5.441	-53.324	–	–	MET509, LEU380, LEU383, PHE384, TYR140, ILE139, VAL311, PHE134	SER508, HIE381, SER382
ML-2	-5.929	-45.601	–	PHE384	LEU383, LEU380, PHE241, PRO238, PHE236	HIE381, SER382
ML-3	-6.526	-48.297	MET509	–	PHE241, LEU380, LEU383, PHE384, TYR140, ILE139, VAL311, VAL510, PHE236, PRO238	HIE381, SER382, SER508
ML-4	-5.723	-43.986	–	PHE384	LEU383, PHE236, TYR140, TYR126, LEU129, PHE241, TYR72	SER382, THR318, HIE381
ML-5	-6.061	-46.437	–	–	LEU380, LEU383, PHE384, VAL311, ILE139, TYR140, LEU129, TYR126, PHE236, PRO238, PHE241	HIE381, SER382, THR318, THR130
ML-6	-5.929	-36.869	TYR126	TYR126	PHE236, VAL311, LEU307, ILE139, TYR140, PHE384, LEU383, LEU380	SER382, THR318
ML-7	-6.353	-50.608	–	–	PHE241, PRO238, PHE236, VAL311, TYR126, LEU129, PHE384, LEU383, LEU380	HIE381, SER382
ML-8	-6.560	-58.839	–	–	MET509, LEU380, LEU383, PHE384, VAL311, ILE139, TYR140, TYR126, LEU129	SER508, HIE381, SER382
ML-9	-6.735	-56.307	–	PHE384, HIE381	PHE506, PRO379, LEU380, LEU383, TYR140, MET509, VAL510	THR507, SER508, THR511, THR318, SER382
ML-10	-5.433	-44.838	–	–	LEU380, LEU383, PHE384, TYR126, LEU129, TYR140, ILE139, PHE134, VAL311	HIE381, SER382, THR130
Fluconazole	-5.092	-60.044	–	HEM601	LEU383, LEU380, TYR126, LEU129, TYR140, ILE139, VAL311	THR130, THR318

ML-6, while π-π stacking interactions involving PHE384 and TYR126 were identified for **ML-2**, **ML-4** and **ML-6** (Fig. 1).

The nature of the aromatic substituents influenced the interaction pattern within the binding site. Nitro-substituted derivatives (**ML-1** and **ML-8**) and halogen-substituted compounds (**ML-2**, **ML-4** and **ML-5**) exhibited favourable hydrophobic and polar contacts, whereas methoxy-containing derivatives displayed aromatic stacking interactions. **ML-8** and **ML-9** showed a balanced combination of hydrophobic and polar interactions, consistent with their superior docking scores. Comparison with fluconazole revealed common interactions with LEU380, LEU383, TYR126, LEU129, TYR140, ILE139 and VAL311, highlighting the importance of these residues in ligand recognition. The docking study provides supportive evidence for the observed antimicrobial activity and offers insight into potential binding modes, although it does not establish direct target inhibition.

Structure activity relationship: The structure–activity relationship analysis of the synthesised thiazole-based Schiff base derivatives (**ML-1** to **ML-10**) revealed that the nature of the aromatic substituents plays an important role in modulating antimicrobial activity. Derivatives containing electron-donating (-OCH_3) and electron-withdrawing (-NO_2) groups exhibited enhanced antibacterial and antifungal effects compared with other analogues. Among the series, **ML-8** and **ML-9** showed the most favourable antimicrobial profiles, which may be associated with the combined influence of the substituted aromatic ring and the 4,5-dihydrothiazol-2-amine propanamide framework. Molecular docking studies identified key interactions with residues LEU380, PHE384, TYR140 and TYR126, involving hydrogen bonding, π-π, stacking and hydrophobic contacts that support ligand stabilization within the binding pocket. Thus, these results highlight the importance of electronic and steric factors in determining biological activity and identify **ML-8** and **ML-9** as suitable candidates for further investigation.

Conclusion

A series of thiazole-based Schiff base derivatives (**ML-1** to **ML-10**) was successfully synthesised and characterised by spectroscopic techniques. The biological evaluation demonstrated moderate antibacterial and antifungal activities among the synthesized compounds, with **ML-9** exhibiting the most favourable activity and MIC values comparable to those of the reference drugs against the tested bacterial strains. Structure activity relationship analysis highlighted the significant influence of electron-donating and electron-withdrawing substituents on the antimicrobial efficacy. Molecular docking studies against the fungal CYP51 enzyme supported the experimental findings, revealing strong binding affinities for **ML-9** and **ML-8** through key interactions with active-site residues. These findings highlight **ML-9** and **ML-8** as potential candidates for further structural optimization and comprehensive biological investigation.

ACKNOWLEDGEMENTS

The authors sincerely thank the Principal, Management and Department of Chemistry at Vivekanand Arts, Sardar

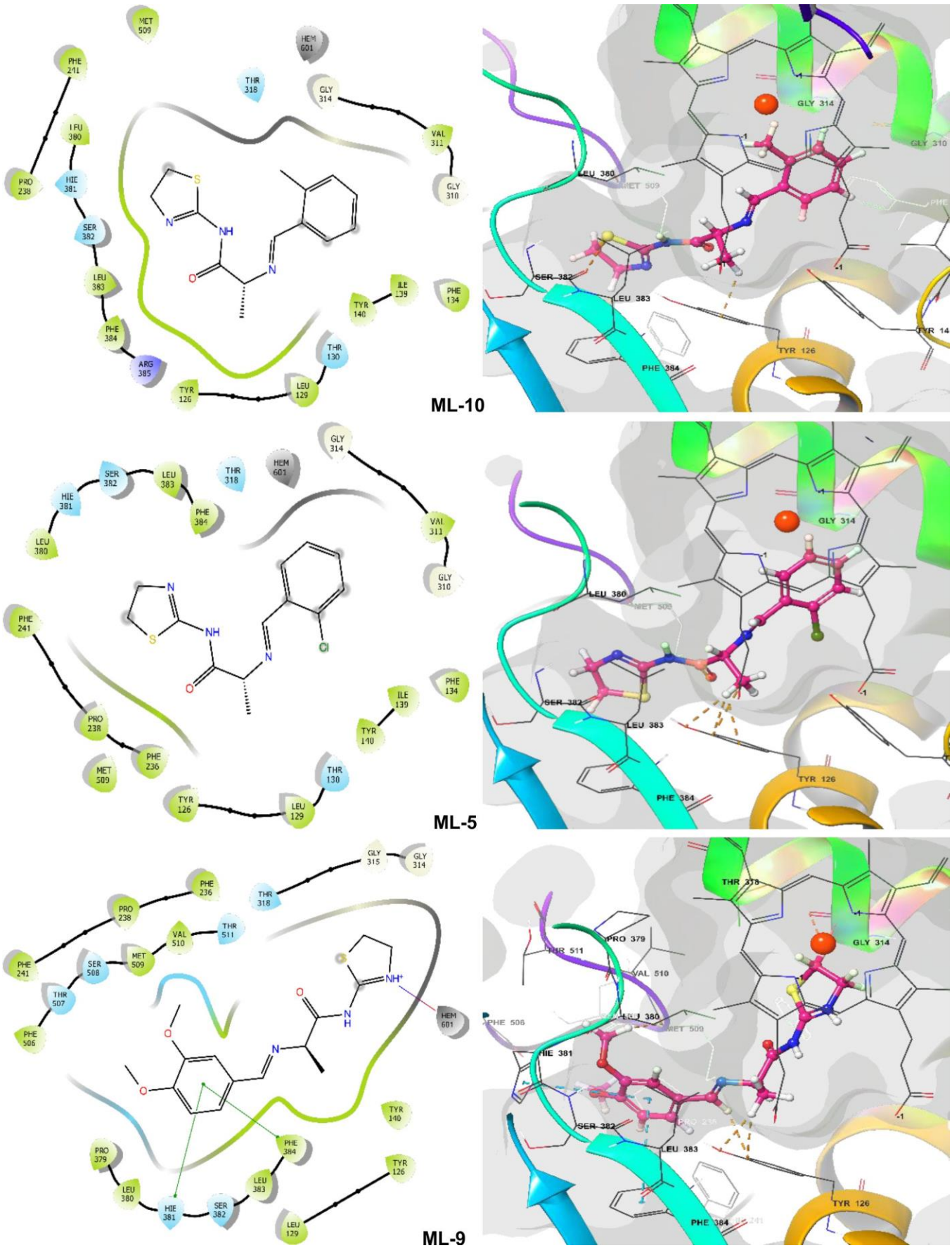

Fig. 2. Docking pose and 2D interactions of compounds **ML-10**, **ML-5** and **ML-9** in cavity of 4WMZ

Dalipsingh Commerce and Science College, Chhatrapati Sambhaji Nagar, India for their support and providing the essential research facilities.

CONFLICT OF INTEREST

The authors declare that there is no conflict of interests regarding the publication of this article.

DECLARATION OF AI-ASSISTED TECHNOLOGIES

During the preparation of this manuscript, the authors used an AI-assisted tool(s) to improve the language. The authors reviewed and edited the content and take full responsibility for the published work.

REFERENCES

1. S. Kumar, A. Arora, S. Sapra, R. Kumar, B.K. Singh and S.K. Singh, *RSC Adv.*, **14**, 902 (2024); https://doi.org/10.1039/D3RA06444A
2. X. Zhou, X. Xu, Y. Li, Z. Zhang and Z.-B. Zheng, *Tetrahedron Lett.*, **57**, 1236 (2016); https://doi.org/10.1016/j.tetlet.2016.02.011
3. M.K. Ibrayev, O.A. Nurkenov, Z.B. Rakhimberlinova, A.T. Takibayeva, I.V. Palamarchuk, D.M. Turdybekov, A.A. Kelmyalene and I.V. Kulakov, *Molecules*, **27**, 7598 (2022); https://doi.org/10.3390/molecules27217598
4. G. Serban, O. Stanasel, E. Serban and S. Bota, *Drug Des Devel Ther.*, **12**, 1545 (2018); https://doi.org/10.2147/DDDT.S155958
5. M.J. Ahsan, J.G. Samy, H. Khalilullah, M.A. Bakht and M.Z. Hassan, *Eur. J. Med. Chem.*, **46**, 3496 (2011); https://doi.org/10.1016/j.ejmech.2011.09.035
6. Ž. Jakopin, *Chem. Biol. Interact.*, **330**, 109244 (2020); https://doi.org/10.1016/j.cbi.2020.109244
7. A.P. Subramanian, R. Samiyappan, B. Anitha, G.K. Ayyadurai and J. Rajendran, *Biomed. Pharmacol. J.*, **17**, 2535 (2024); https://doi.org/10.13005/bpj/3046
8. S. Ejaz, H. Nadeem, R.Z. Paracha, S. Sarwar and S. Ejaz, *BMC Chem.*, **13**, 115 (2019); https://doi.org/10.1186/s13065-019-0631-6
9. R.K.P. Tripathi, V.M. Sasi, S.K. Gupta, S. Krishnamurthy and S.R. Ayyannan, *J. Enzyme Inhib. Med. Chem.*, **33**, 37 (2018); https://doi.org/10.1080/14756366.2017.1389920
10. F. Lemilemu, M. Bitew, T. B. Demissie, R. Eswaramoorthy and M. Endale, *BMC Chem.*, **15**, 67 (2021); https://doi.org/10.1186/s13065-021-00791-w
11. M.F. Elsadek, B.M. Ahmed and M.F. Farahat, *Molecules*, **26**, 1449 (2021); https://doi.org/10.3390/molecules26051449
12. A. Petrou, V. Kartsev, A. Geronikaki, J. Glamočlija, A. Ćirić and M. Soković, *SAR QSAR Environ. Res.*, **34**, 395 (2023); https://doi.org/10.1080/1062936X.2023.2214869
13. A. Pandey, R. Rajavel, S. Chandraker and D. Kumar, *J. Chem.*, **9**, 2524 (2012); https://doi.org/10.1155/2012/145028
14. P.J. Wallis, W.P. Gates, A.F. Patti, J.L. Scott and E. Teoh, *Green Chem.*, **9**, 980 (2007); https://doi.org/10.1039/B701504F
15. H. Naeimi, F. Salimi and K. Rabiei, *J. Mol. Catal. A: Chem.*, **260**, 100 (2006); https://doi.org/10.1016/j.molcata.2006.06.055
16. G. Fan, F. Li, D.G. Evans and X. Duan, *Chem Soc. Rev.*, **43**, 7040 (2014); https://doi.org/10.1039/C4CS00160E
17. J. Zhu, L. Chen, H. Wu and J. Yang, *Chin. J. Chem.*, **27**, 1868 (2009); https://doi.org/10.1002/cjoc.200990313
18. L. Ravishankar, S. A. Patwe, N. Gosarani and A. Roy, *Synth. Commun.*, **40**, 3177 (2010); https://doi.org/10.1080/00397910903370725
19. P. Bedi, M. Lalit, R. Gupta and T. Pramanik, *Res. J. Chem. Environ.*, **22**, 19 (2018).
20. S.B. Manjare, R.K. Mahadik, K.S. Manval, P.P. More and S.S. Dalvi, *ACS Omega*, **8**, 473 (2022); https://doi.org/10.1021/acsomega.2c05187
21. P. Vinoth Kumar and G. Madhumitha, *RSC Adv.*, **14**, 4810 (2024); https://doi.org/10.1039/D3RA06358E
22. B.S. Kumar, A. Dhakshinamoorthy and K. Pitchumani, *Catal. Sci. Technol.*, **4**, 2378 (2014); https://doi.org/10.1039/C4CY00112E
23. K. Campbell, C. Helbing, M. Florkowsk and B. Campbell, *J. Am. Chem. Soc.*, **70**, 3868 (1948); https://doi.org/10.1021/ja01191a099
24. S. Magaldi, C. Mata-Essayag, C. Capriles, C. Perez, M. Colella, C. Olaizola and Y. Ontiveros, *Int. J. Infect. Dis.*, **8**, 39 (2004); https://doi.org/10.1016/j.ijid.2003.03.002
25. H.M. Abosalim, M.A. Nael and T.F. El Moselhy, *ChemistrySelect*, **6**, 888 (2021); https://doi.org/10.1002/slct.202004088
26. E. Valeur and M. Bradley, *Chem. Soc. Rev.*, **38**, 606 (2009); https://doi.org/10.1039/B701677H
27. K.M. Engstrom, Org. Process Res. Dev., **22**, 1294 (2018); https://doi.org/10.1021/acs.oprd.8b00121
28. E.A. Khachatryan, L.A. Stepanyan, H.R. Gevorgyan, A.S. Sargsyan, A.M. Hovhannisyan, A.F. Mkrtchyan, A.V. Malkov and A.S. Saghyan, *Org. Biomol. Chem.*, **24**, 465 (2026); https://doi.org/10.1039/D5OB01593F